One-dimensional continuous analytic potential solution to generic oxide–silicon–oxide system*

Zhang Jian(张 健)[a], He Jin(何 进)[a)b)†], and Zhang Li-Ning(张立宁)[a)]

[a)] *Institute of Microelectronics, School of Electronic Engineering and Computer Science, Peking University, Beijing* 100871, *China*

[b)] *The Key Laboratory of Integrated Microsystems, School of Computer & Information Engineering, Peking University Shenzhen Graduate School, Shenzhen* 518055, *China*

(Received 1 June 2009; revised manuscript received 6 December 2009)

A one-dimensional continuous analytic potential solution to a generic oxide–silicon–oxide system is developed. With the analytic solution, the potential distribution in the silicon film is predicted. A physics-based relation between surface potentials is also derived and then applied to the generic oxide–silicon–oxide metal–oxide–semiconductor field-effect transistors (MOSFETs) for the calculation of surface potentials

Keywords: surface potential, MOSFET modeling, oxide–silicon–oxide system

PACC: 7340, 7340Q, 7340T

1. Introduction

Interest in the development of compact models for silicon-on-insulator (SOI) and double-gate (DG) metal–oxide–semiconductor field-effect transistors (MOSFETs) has increased considerably recently.[1−3] Nevertheless, a unified understanding of the generic oxide–silicon–oxide system has not been available so far.[4,5] In this paper, a continuous analytic potential solution to the generic oxide–silicon–oxide system is developed. With the fixed point method, the potential distribution in the silicon film is predicted. A relation between the surface potentials is also derived and then applied to SOI/DG MOSFETs to calculate the surface potentials from the accumulation region to the strong inversion region.

2. Solution derivation

As a generic oxide–silicon–oxide system, two gates with different gate bias and geometry parameters are assumed. For a P-type silicon body in an oxide–silicon–oxide system, one-dimensional Poisson–Boltzmann's equation perpendicular to the interface between the oxide and the silicon film is written as

$$\frac{\mathrm{d}^2\phi}{\mathrm{d}x^2} = \frac{qN_\mathrm{A}}{\varepsilon_\mathrm{si}}\left[1 - \mathrm{e}^{(-2\phi_\mathrm{F}-V)/V_t} + \mathrm{e}^{(\phi-2\phi_\mathrm{F}-V)/V_t} - \mathrm{e}^{-\phi/V_t}\right], \tag{1}$$

where ϕ is the electrostatic potential, q is the elementary charge, N_A is the silicon doping concentration, ε_si is the silicon permittivity, $V_t \equiv k_\mathrm{B}T/q$ is the thermal voltage, with k_B being the Boltzmann constant, T the absolute temperature, and $\phi_\mathrm{F} = V_t \ln(N_\mathrm{A}/n_\mathrm{i})$ is the Fermi potential with n_i the intrinsic carrier concentration, and V is the quasi-Fermi potential.

A general solution to Eq. (1) is derived by integrating Eq. (1) twice thus yielding

$$\begin{aligned}\phi - \phi_\mathrm{sb} = {} & q_\mathrm{b}\left[\left(1 - \mathrm{e}^{(-2\phi_\mathrm{F}-V)/V_t}\right)(1-t)^2 \right. \\ & \left. + \lambda_1(t)\,\mathrm{e}^{(\phi_\mathrm{sb}-2\phi_\mathrm{F}-V)/V_t} - \lambda_2(t)\,\mathrm{e}^{-\phi_\mathrm{sb}/V_t}\right] \\ & + E_\mathrm{b}t_\mathrm{si}(1-t),\end{aligned} \tag{2}$$

where t_si is the thickness of the silicon film, $q_\mathrm{b} = qN_\mathrm{A}t_\mathrm{si}^2/2\varepsilon_\mathrm{si}$, $\phi_\mathrm{sb} \equiv \phi(x = t_\mathrm{si})$ is the electrostatic potential at the back surface of the silicon film as the reference point, E_b is the electric field at the reference point, which is determined by the boundary condition with Gauss's law. And

$$\lambda_1(t) = 2\int_t^1\int_v^1 \mathrm{e}^{(\phi-\phi_\mathrm{sb})/V_t}\,\mathrm{d}u\,\mathrm{d}v, \tag{3a}$$

$$\lambda_2(t) = 2\int_t^1\int_v^1 \mathrm{e}^{-(\phi-\phi_\mathrm{sb})/V_t}\,\mathrm{d}u\,\mathrm{d}v \tag{3b}$$

with $t, u, v = x/t_\mathrm{si}$ being the normalized coordinates.

*Project supported by the National Natural Science Foundation of China (Grant Nos. 60876027 and 60976066), and the National Science Fund for Distinguished Young Scholars of China (Grant No. 60925015).

†Corresponding author. E-mail: frankhe@pku.edu.cn

© 2010 Chinese Physical Society and IOP Publishing Ltd

Equation (2) together with Eq. (3) cannot be expressed by a rigorously analytic solution. But with a fixed-point method, an approximate solution is obtained. Note that equation (2) is an equation of the form $p = g(p)$ where $p = \phi - \phi_{\rm sb}$, its root can be approached by the sequence p_1, p_2, ..., calculated by $p_{n+1} = g(p_{\rm n})$ starting from a fixed-point p_0. To obtain an analytical solution of Eq. (2), this iteration is just repeated analytically once or twice in our work with a good initial guess. This process is very similar to the fixed-point iteration method in the numerical analysis and the convergence is ensured since equation (2) satisfies the Lipschitz condition.[6,7]

The analytical approximation starts from a rough initial solution guess $\phi - \phi_{\rm sb} = 0$ called the local approximation. With this fixed-point solution, equations (3a) and (3b) are simply written as

$$\lambda_1(t) = \lambda_2(t) = (1-t)^2. \tag{4}$$

A more accurate solution for $\phi - \phi_{\rm sb}$ is obtained by substituting Eq. (4) into the terms on the right-hand side of Eq. (2),

$$\phi - \phi_{\rm sb} = q_{\rm b}\left(1 - {\rm e}^{(-2\phi_{\rm F}-V)/V_t} + {\rm e}^{(\phi_{\rm sb}-2\phi_{\rm F}-V)/V_t} - {\rm e}^{-\phi_{\rm sb}/V_t}\right)(1-t)^2 + E_{\rm b}t_{\rm si}(1-t). \tag{5}$$

Thus, solution (6) which is closer to the root of Eq. (2) is developed by substituting Eq. (5) into Eqs. (3a) and (3b) again

$$\lambda_1(t) = \frac{1}{a}\left\{1 - \exp(c_0) + c_1\sqrt{\pi}\exp\left(-c_2^2\right)\left[{\rm erfi}(c_1) - {\rm erfi}(c_2)\right]\right\}, \tag{6a}$$

$$\lambda_2(t) = \frac{1}{a}\left\{-1 + \exp(-c_0) + c_1\sqrt{\pi}\exp\left(c_2^2\right)\left[{\rm erf}(c_1) - {\rm erf}(c_2)\right]\right\}, \tag{6b}$$

where $a = q_{\rm b}\left[1 - {\rm e}^{(-2\phi_{\rm F}-V)/V_t} + {\rm e}^{(\phi_{\rm sb}-2\phi_{\rm F}-V)/V_t} - {\rm e}^{-\phi_{\rm sb}/V_t}\right]/V_t$, $b = E_{\rm b}t_{\rm si}/V_t$, $c_0 = a(1-t)^2 + b(1-t)$, $c_1 = b/(2\sqrt{a}) + \sqrt{a}(1-t)$, $c_2 = b/(2\sqrt{a})$ and erfi(x) is the imaginary error function, erf(x) is the error function.

With this potential distribution relation, once the potential at the reference point is known, the potential distribution in the silicon film is also predicted from Eq. (2) as shown in Fig. 1.

In the development of the compact model, the solution of surface potentials is usually important. Applying Eq. (2) to the DG/SOI MOSFET structure, the relationship between surface potentials $\phi_{\rm sf}$ and $\phi_{\rm sb}$ is expressed as

$$\begin{aligned}&\phi_{\rm sf} - \phi_{\rm sb}\\ &= q_{\rm b}\left[1 - {\rm e}^{(-2\phi_{\rm F}-V)/V_t} + \lambda_1(0)\,{\rm e}^{(\phi_{\rm sb}-2\phi_{\rm F}-V)/V_t}\right.\\ &\quad\left. - \lambda_2(0)\,{\rm e}^{-\phi_{\rm sb}/V_t}\right] + E_{\rm b}t_{\rm si}.\end{aligned} \tag{7}$$

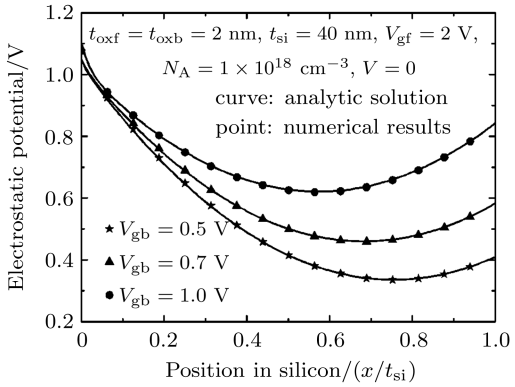


Fig. 1. Plot of the electrostatic potential distribution in an oxide–silicon–oxide structure.

On the other hand, the surface potential is calculated by combining with the well-known equation[4]

$$\begin{aligned}E_{\rm f}^2 - E_{\rm b}^2 = \frac{2qN_{\rm A}}{\varepsilon_{\rm si}}&\left\{{\rm e}^{(-2\phi_{\rm F}-V)/V_t}\left[V_t\left({\rm e}^{\phi_{\rm sf}/V_t} - {\rm e}^{\phi_{\rm sb}/V_t}\right) - (\phi_{\rm sf} - \phi_{\rm sb})\right]\right.\\ &\left. + V_t\left({\rm e}^{-\phi_{\rm sf}/V_t} - {\rm e}^{-\phi_{\rm sb}/V_t}\right) + (\phi_{\rm sf} - \phi_{\rm sb})\right\},\end{aligned} \tag{8}$$

where $E_{\rm f}$ and $E_{\rm b}$ are the surface electric fields given by Gauss's law

$$E_{\rm f} = \frac{C_{\rm oxf}(V_{\rm gf} - \phi_{\rm sf})}{\varepsilon_{\rm si}},$$

and

$$E_{\rm b} = \frac{C_{\rm oxb}(\phi_{\rm sb} - V_{\rm gb})}{\varepsilon_{\rm si}}$$

with $C_{\rm oxf(oxb)} = \varepsilon_{\rm ox}/t_{\rm oxf(oxb)}$ being the front-gate/back-gate oxide capacitance, and $V_{\rm gf/gb}$ the effective front-gate/back-gate voltage, respectively.

The equation group of Eqs. (7) and (8) is solved by using the Newton–Raphson method, thereby yielding the surface potentials $\phi_{\rm sf}$ and $\phi_{\rm sb}$. The obtained surface potentials are shown in Fig. 2.

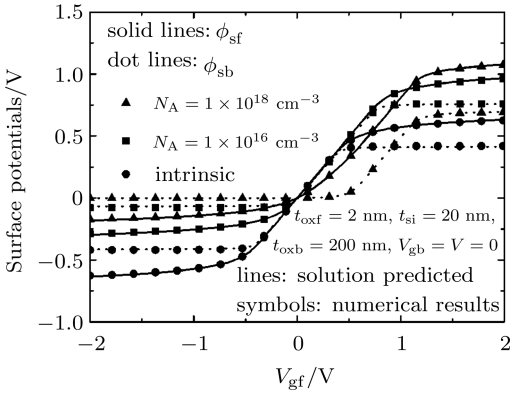


Fig. 2. Plot of the surface potentials from accumulation to strong inversion in an SOI MOSFET.

3. Results and discussion

Figure 1 shows the potential distribution in the silicon film in an oxide–silicon–oxide structure, and figure 2 plots the surface potentials versus $V_{\rm gf}$ from accumulation to strong inversion for an SOI MOSFET. The analytical results show good agreement with the numerical simulations.[8] It is verified that the algorithm is sufficiently robust for a large range of gate voltages and geometry parameters. From Eq. (2), it is evident that the obtained potential relation can describe both the monotonic and the non-monotonic distributions, depending on the boundary, e.g. the sign of $E_{\rm b}$. Figures 1 and 2 with different boundary conditions prove that well.

We also proposed approximation (5) for $\phi - \phi_{\rm sb}$ with simpler formulation and higher computing efficiency. The practical test shows that approximation (5) also has a high accuracy for the calculation of $\phi_{\rm sf}$, and just a small error of $\phi_{\rm sb}$ appears in the strong inversion region.[7]

Figure 3 shows the gate charge density $Q_{\rm gf}$ as a function of gate voltage. There are four distinct operation regions in SOI MOSFETs, i.e. the accumulation region, the partially depleted (PD) region, the coupling region, and the strong inversion region. The coupling region appears only when the body is fully depleted (FD), which is quite different from the conventional bulk MOSFETs. Due to the fact that both the electron and the hole are considered in the complete Poisson–Boltzmann's equation, thus, the obtained solution is continuous and smooth from the accumulation region to the strong inversion region. On the other hand, the dynamic depletion of the SOI MOSFETs is perfectly captured by the developed solution without any smooth function or fitting parameter.

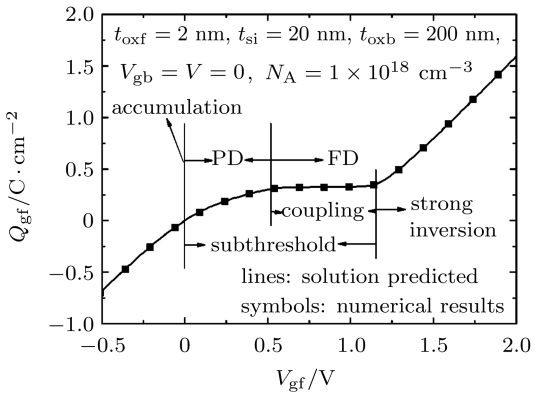


Fig. 3. Front-gate charge densities in different operation regions in a dynamic-depletion SOI MOSFET.

4. Conclusions

In this paper, a one-dimensional continuous analytic potential solution to a generic oxide–silicon–oxide system is developed. The presented solution not only is valid to predict both the monotonic and non-monotonic potential distributions in the silicon film, but also captures the dynamic depletion characteristics of DG/SOI MOSFETs. The proposed solution is also quite suitable to the calculation of the surface potentials from the accumulation to the strong inversion region.

References

[1] Taur Y 2001 *IEEE Trans. Electron Devices* **48** 2861

[2] Liu H X and Luan S Z 2008 *Chin. Phys.* B **17** 3077

[3] Hu S D, Li Z J and Zhang B 2009 *Chin. Phys.* B **18** 315

[4] Sleight J W and Rios R 1998 *IEEE Trans. Electron Devices* **45** 821

[5] Shi X and Wong W 2003 *IEEE Trans. Electron Devices* **50** 1793

[6] Conte S D and Carl de Boor 1980 *Elementary Numerical Analysis: an Algorithmic Approach* (New York: McGraw-Hill)

[7] Liu F, He J, Zhang J, Chen Y and Chan M 2008 *IEEE Trans. Electron Devices* **55** 3494

[8] Synopsys 2005 *TCAD Sentaurus Device User's Manual* (CA: Mountain View)